Wnt Signaling Drives Ectopic Gene Expression and Larval Arrest in the Absence of the *Caenorhabditis elegans* DREAM Repressor Complex

Jerrin R. Cherian, Katherine V. Adams, and Lisa N. Petrella[1]

Department of Biological Sciences, Marquette University, Milwaukee, WI 53233

ORCID ID: 0000-0001-8664-7435 (L.N.P.)

ABSTRACT Establishment and maintenance of proper gene expression is a requirement for normal growth and development. The DREAM complex in *Caenorhabditis elegans* functions as a transcriptional repressor of germline genes in somatic cells. At 26°, DREAM complex mutants show increased misexpression of germline genes in somatic cells and High Temperature Arrest (HTA) of worms at the first larval stage. To identify transcription factors required for the ectopic expression of germline genes in DREAM complex mutants, we conducted an RNA interference screen against 123 transcription factors capable of binding DREAM target promoter loci for suppression of the HTA phenotype in *lin-54* mutants. We found that knock-down of 15 embryonically expressed transcription factors suppress the HTA phenotype in *lin-54* mutants. Five of the transcription factors found in the initial screen have associations with Wnt signaling pathways. In a subsequent RNAi suppression screen of Wnt signaling factors we found that knock-down of the non-canonical Wnt/PCP pathway factors *vang-1*, *prkl-1* and *fmi-1* in a *lin-54* mutant background resulted in strong suppression of the HTA phenotype. Animals mutant for both *lin-54* and *vang-1* showed almost complete suppression of the HTA phenotype, *pgl-1* misexpression, and fertility defects associated with *lin-54* single mutants at 26°. We propose a model whereby a set of embryonically expressed transcription factors, and the Wnt/PCP pathway, act opportunistically to activate DREAM complex target genes in somatic cells of DREAM complex mutants at 26°.

Properly regulated gene expression is critical for normal growth and development of an organism. In metazoan development, embryonic cells become either totipotent germ cells, or somatic cells that undergo cell fate specification and differentiation. Consequently, somatic cells must repress the gene expression program associated with germline cells. Misregulation of gene expression control is associated with altered cell-fate specification, which can lead to retarded development or cancer (Gross *et al.* 2016; Smith *et al.* 2019). For example, hundreds of genes expressed primarily in germ cells (germline genes) are up-regulated in 19 different somatic cancers (Wang *et al.* 2016). Evidence suggests that germline genes can drive cancer acquisition and progression (Chang *et al.* 2019). To maintain correct cell fate, precise control of both spatial and temporal gene expression is required via a network of transcriptional activators and repressors (Kudron *et al.* 2013).

In *C. elegans*, the DREAM complex alters chromatin structure in the nucleus to transcriptionally repress germline genes in somatic cells (Costello and Petrella 2019; Cui *et al.* 2006; Latorre *et al.* 2015; Petrella *et al.* 2011; Rechtsteiner *et al.* 2019; Unhavaithaya *et al.* 2002; Wang *et al.* 2005; Wu *et al.* 2012). The DREAM complex is completely conserved between mammals and *C. elegans*, and comprised of eight proteins: E2F-DP heterodimer (EFL-1 and DPL-1), a retinoblastoma-like pocket protein (LIN-35), and a 5-subunit MuvB complex (LIN-9, LIN-37, LIN-52, LIN-53, and the DNA binding subunit LIN-54) (Goetsch *et al.* 2017; Harrison *et al.* 2006; Latorre *et al.* 2015; Sadasivam and DeCaprio 2013). In *C. elegans*, a mutant form of

LIN-54 is incapable of binding the majority of DREAM complex target loci due to a change in a single amino acid in the DNA binding motif (Tabuchi *et al.* 2011). A putative null allele of *lin-35*, which physically mediates the interaction between the E2F-DP dimer and MuvB subcomplex, results in reduced DREAM complex binding to target loci and reduced repression capability of the DREAM complex (Goetsch *et al.* 2017). Germline genes, such as that encoding the germline specific P-granule component PGL-1, are inherently expressed only in the germline with no detectable expression in somatic cells (Pitt *et al.* 2000). Mutation in *lin-54*, *lin-35*, and several other members of the DREAM complex members results in low level misexpression of *pgl-1* in somatic cells at 20° (Wang *et al.* 2005) and increased misexpression under moderate temperature stress of 26° (Petrella *et al.* 2011). Ectopic P-granule expression in the intestine of DREAM complex mutants is correlated with the High Temperature Larval Arrest (HTA) phenotype, where worms grown at 26° developmentally arrest at the L1 larval stage (Petrella *et al.* 2011).

Wild-type embryonic development is characterized by rapid chromatin compaction, with cells achieving closed chromatin structures between the 100 to 200 cell stage (Mutlu *et al.* 2018). While wild-type embryos show a moderate delay in this process at high temperature; DREAM complex mutants at high temperature show severe delays in the chromatin compaction process. This delay results in open chromatin persisting later in development, most prominently in anterior embryonic intestinal cells (Costello and Petrella 2019). Open chromatin structures have been shown to facilitate recruitment of DNA binding proteins such as transcription factors (Heinz and Glass 2012). Transcription factors act both spatially and temporally within the chromatin landscape to modulate gene expression (Li and Leonard 2018; Praggastis and Thummel 2017). Repressor complexes, such as the DREAM complex, work antagonistically to gene activation by preventing RNA polymerase access to target promoter loci (Hernández-Arriaga *et al.* 2009). The delayed chromatin compaction seen in DREAM complex mutants may provide an opportunity for transcription factors to ectopically activate germline genes in the soma. Additionally, the A-P pattern of decreased chromatin compaction in DREAM complex mutants suggests a role for cell-signaling pathways involved in embryonic A-P patterning in promoting ectopic germline gene expression. Neither the transcription factors nor cell signaling pathways necessary for ectopic germline gene expression in DREAM complex mutants are known.

In this study, we conducted an RNAi screen of 123 transcription factors (TFs) that were predicted to bind DREAM target loci and scored for suppression of HTA in *lin-54* mutants. We found that knock-down of 15 of the transcription factors resulted in suppression of the HTA phenotype in *lin-54* mutants. Knockdown of nine of 15 TF HTA suppressors was also able to suppress the ectopic expression of the germline gene PGL-1 in *lin-54* mutants. Signaling pathway enrichment analysis of the HTA transcription factor suppressors showed significant enrichment of the Wnt signaling pathway, one of the primary A-P patterning signaling pathways in *C. elegans*. We therefore performed RNAi of Wnt pathway components for their ability to suppress the HTA phenotype in *lin-54* mutants. While loss of a number of Wnt components suppressed the HTA phenotype, knock-down of Wnt/PCP pathway members, including *vang-1*, showed strong suppression of HTA. *lin-54*; *vang-1* double mutants showed complete suppression of HTA phenotype and reduced ectopic PGL-1 expression to baseline levels. Loss of *vang-1* also completely suppressed the fertility defects seen in *lin-54* mutants. We propose that the Wnt/PCP pathway

can act to promote gene expression in both the soma and germline in the absence of DREAM complex.

MATERIALS AND METHODS

Strains and nematode culture

C. elegans were cultured under standard conditions (Brenner 1974) on NGM plates seeded with *E. coli* strain AMA1004 at 20° unless otherwise noted. N2 (Bristol) was used as wild-type. Mutant strains used for the experiments were MT8841 *lin-54(n2231)*, MT10430 *lin-35(n745)*, MT8838 *lin-13(n770)*, RB1125 vang-1(ok1142), LNP0073 *lin-54(n2231);vang-1(ok1142)*, CF1045 *muIs49 [unc-22(+), Pegl-20::egl-20::GFP]*, and LNP0096 *lin-54(n2231);muIs49 [unc-22(+), Pegl-20::egl-20::GFP]*. All strains, except LNP0073 and LNP0096 which were made for this study, were provided by the CGC, which is funded by NIH Office of Research Infrastructure Programs (P40 OD010440).

Selection of transcription factor candidates for RNAi screen

The Yeast-1-Hybrid (Y1H) Assay dataset (Reece-Hoyes *et al.* 2011) was used to obtain a list of transcription factors (TFs) to screen for suppression of HTA phenotype in *lin-54* mutants. This dataset includes the interactions of 296 predicted transcription factors (Fuxman Bass *et al.* 2016) as prey screened to interact with 534 promoter loci bait sequences (Reece-Hoyes *et al.* 2011). We found that 46 bait sequences in the Y1H dataset were known to be bound by the DREAM complex in their promoter region in late embryos (Goetsch *et al.* 2017). We found that 123 of the 296 TFs showed binding to at least one of the 46 DREAM target promoter loci in the Y1H data set (Table S1). These 123 TFs were used as candidates in the transcription factor RNAi screen.

Suppression of High Temperature Larval Arrest (HTA) phenotype assay

Hermaphrodites were maintained at 20° on NGM plates with AMA1004 bacteria until the L4 larval stage. At the L4 larval stage P0 worms were moved to plates containing transcription factor (TF) specific RNAi feeding bacteria NGM (0.2% lactose, 0.075 mg/ml ampicillin), and simultaneously upshifted to 26°. After ~18 hr the P0 worms were moved to new RNAi plates and allowed to lay embryos for 24 hr. For preliminary qualitative HTA suppression RNAi screen, each RNAi plate was scored as either primarily having F1 worms that were arrested at the L1 stage or primarily having worms that grew beyond L1 stage. For quantitative HTA suppression RNAi screen against TF and Wnt signaling components, individual F1 worms were counted either as arrested at L1 stage or growing to the L4/Adult stage. Worms grown on empty L4440 vector containing bacteria was used as a RNAi negative control. RNAi against *mrg-1*, a chromatin modifier previously shown to suppress HTA in DREAM mutants (Petrella *et al.* 2011), was used as a positive control. For suppression of HTA phenotype assay in *lin-54*; *vang-1* mutants, the assay was performed as described above except that worms were grown on regular NGM plates seeded with AMA1004 throughout the assay. Statistical significance was determined by comparing test samples with negative control using Fishers Exact test in Graph Pad Prism.

Immunostaining

L4 stage worms were upshifted to 26° on RNAi feeding bacteria containing plates as described above. On the next day, gravid adult worms from these plates were placed in 100μL M9 buffer on a slide in a humid chamber at 26° to lay embryos. L1 worms were placed on a poly-L-lysine-coated slide and a coverslip was placed over the

sample. Excess M9 buffer was wicked away and the slide was placed in liquid nitrogen for a minimum of five minutes. Slides were freeze cracked and fixed in cold methanol for 10 min followed by cold acetone for 10 min each. Slides were air dried and blocked for an hour with 1.5% of Bovine Serum Albumin and 1.5% of Ovalbumin in PBS (adapted from Strome and Wood 1983). Polyclonal rabbit anti-PGL-1 antibody (Kawasaki *et al.* 1998) was used at 1:10,000 dilution overnight at 4°. Slides were washed three times in PBS for 10 min and blocked for 15 min at room temperature. Slides were incubated with secondary antibody conjugated to Alexa Fluor 647 (Thermofisher Scientific, Cat No. A-21244) at 1:500 dilution for 2 hr at room temperature. Slides were treated with 5mg/ml DAPI in 50 mL PBS for 10 min, washed 3 times with PBS for 10 min at room temperature and mounted on gelutol mounting medium. Z-stacks were taken using Nikon A1R Inverted Microscope Eclipse T*i* confocal microscope with NIS Elements AR 3.22.09 at 60X. PGL-1 quantification was done in NIS-Elements Analysis program. First, all somatic cells were outlined to separate them from primordial germ cells to create a region of interest. Second, the mean somatic PGL-1 intensity for each worm was obtained using the ROI statistics function. The adjusted PGL-1 intensity was calculated by subtracting a worm's mean PGL-1 pixel intensity from the mean background pixel intensity and then dividing the result by mean background pixel intensity (Zhao *et al.* 2018). Statistically significant difference between test samples and L4440 empty vector negative control was calculated using Kolmogorov-Smirnov test in Graph Pad Prism. In the case of *lin-54; vang-1* mutants, worms were grown on regular NGM plates seeded with AMA1004 and the staining and analysis were performed as described above.

Gene ontology enrichment analysis

Gene Ontology Analysis was performed using two different enrichment analysis tools: gProfiler - https://biit.cs.ut.ee/gprofiler/gost (Version: e96_eg43_p13_563554d) (Raudvere *et al.* 2019) and PANTHER Overrepresentation Test - http://geneontology.org/ (Release: 20190711) (Ashburner *et al.* 2000; Mi *et al.* 2019). Transcription factor candidates with significant HTA suppression in *lin-54* mutants were uploaded to both the enrichment analysis tools and the significantly enriched ontology terms were obtained (Multiple testing correction: PANTHER - FDR < 0.05; gProfiler - Custom g:SCS Set Counts and Sizes correction method, Cut off value:0.05).

Brood size assay

The brood size of worms was determined at 3 different temperature conditions, 20°, up-shift from 20° to 26° at the L4 stage, and 26°. For 20°, individual P0 hermaphrodites were placed on a plate starting at the L4 stage and moved to a new plate every 24 hr until the worms stopped having progeny. The total number of F1 progeny for each P0 worm was counted. For upshifting, P0 hermaphrodites were maintained at 20° until the L4 stage and then shifted to 26° at the L4 stage on individual plates. The worms were moved to a different plate every 24 hr until the worms stopped having progeny. The total number of F1 progeny for each P0 hermaphrodite were counted. For 26°, P0 hermaphrodites were maintained at 20° until the L4 stage and then shifted to 26° and allowed to have progeny. The F1 progeny that had grown continuously at 26° were placed on an individual plate at the L4 stage and moved to a new plate every 24 hr until the worms stopped having progeny. The total number of F2 progeny for each F1 worm was counted. Brood sizes of zero were excluded. Statistical analysis of brood size was done using Welch's T test on fertile animals using Graph Pad Prism.

EGL-20::GFP expression analysis

L4 stage worms were used at 20° or upshifted to 26° on NGM plates containing AMA1004 bacteria. On the next day, gravid adult worms from these plates were placed in 100μL M9 buffer on a slide in a humid chamber at either 20° or 26° to lay embryos. L1 worms were moved to a poly-L-lysine-coated slide and a coverslip was placed over the sample. M9 buffer present in excess was wicked away and the slide was kept in liquid nitrogen for a minimum of five minutes. Slides were freeze cracked, and fixed in cold methanol for 10 min followed by cold acetone for 10 min each (adapted from Strome and Wood,1983). Slides were treated with 5 mg/ml DAPI in 50 mL PBS for 10 min, washed 3 times with PBS for 10 min at room temperature and mounted on gelutol mounting medium. Z-stacks were taken using Nikon A1R Inverted Microscope Eclipse T*i* confocal microscope with NIS Elements AR 3.22.09 at 60X. To determine the area along the A-P axis where EGL-20::GFP was expressed, we drew a polygonal line using measure length function under the annotation and measurement function of NIS Elements Analysis program. The length of the EGL-20:GFP area on the dorsal side of the worm was determined by starting the measurement from the point where GFP pixel intensity increased above the background GFP pixel intensity and continued until the GFP pixel intensity returned to the background GFP pixel intensity at the same level as at the start of the line. The length of the entire worm was determined by manually drawing a line along the length of the dorsal side of the worm. The same analysis was performed on the ventral side of the worm. Statistical analysis was done using Students T test using Graph Pad Prism.

Data availability

All strains and noncommercially available reagents are available upon request. Figure S1 contains HTA suppression data for TF knockdown in *lin-54* mutants for TF candidates that passed the preliminary binary qualitative screen but failed the quantitative analysis. Figure S2 contains distribution of adjusted PGL-1 intensity data for wild type and *lin-54* mutant controls at both 20° and 26°. Figure S3 contains Quantification of Wnt ligand EGL-20 localization in *lin-54* mutants. Table S1 contains the list of TFs with DREAM target loci binding information. Table S2 shows a list of transcription factors tested for suppression of HTA phenotype in *lin-54* mutants and the TF families. Table S3 contains a list of enriched GO terms, Wiki Pathway terms and TransFac terms determined using gProfiler for TFs that show significant suppression of the HTA phenotype in *lin-54* mutants. Table S4 contains a list of enriched GO terms determined using PANTHER Overrepresentation test for TFs that show significant suppression of the HTA phenotype in *lin-54* mutants. Table S5 contains a list of Wnt signaling genes that were tested for suppression of HTA phenotype in *lin-54* mutants. Supplemental material available at figshare: https://doi.org/10.25387/g3.11320484.

RESULTS

Multiple transcription factors are required for the high temperature larval arrest phenotype of lin-54 mutants

Loss of the DREAM complex results in up-regulation of many genes including ectopic somatic expression of genes normally only expressed in the germline (Petrella *et al.* 2011, Wang *et al.* 2005, Wu *et al.* 2012). The up-regulation of DREAM target genes in DREAM complex mutants correlates with the High Temperature larval Arrest (HTA) phenotype, characterized by a developmental arrest at the L1 stage when animals are grown at 26° (Petrella *et al.* 2011). We predicted that ectopic expression of DREAM target genes in DREAM mutants likely

requires the activity of transcription factors (TFs) (Figure 1a). To find the TFs necessary for driving ectopic expression of DREAM target genes, we performed an RNAi knockdown screen of TFs in *lin-54* mutants for suppression of the HTA phenotype. For our screen, we used a hypomorphic *lin-54*(n2231) allele, as it limits DREAM complex DNA binding but is healthy and fertile (Tabuchi *et al.* 2011). To limit the screen to TFs that directly bind to and regulate DREAM complex targets, we developed a candidate set of 123 TFs from those shown to bind DREAM targets *in vitro* by Yeast-1-Hybrid (Table S1)(Reece-Hoyes *et al.* 2011). For the initial screen, we performed RNAi against 123 TFs in *lin-54* mutants at 26° and screened for the suppression of the HTA phenotype using a binary (yes/no) method where plates were scored for the presence of L4/adults worms (Figure 1b). As a positive control, we performed RNAi against *mrg-1*, a chromatin associated factor previously shown to suppress the HTA phenotype (Petrella *et al.* 2011). We found that RNAi against 26 of 123 TF candidates tested were able to suppress the HTA phenotype in *lin-54* mutants (Table S2). We retested those 26 TFs by quantifying the percentage of worms that grew to the L4/adult stage. RNAi against 15 of 26 TFs (henceforth called TF HTA suppressors) showed statistically significant suppression of HTA in *lin-54* mutants compared to the empty vector L4440 RNAi control (Figure 1c, Table 1, Figure S1). The TF HTA suppressors fell into three transcription factor DNA binding domain families: homeodomain (HD), Winged Helix (WH), and zinc finger (ZF) (Table 1).

TF HTA suppressors are required for the HTA phenotype of lin-35 mutants but not lin-13 mutants

Loss of *lin-35*, the sole Retinoblastoma homolog DREAM complex member in *C. elegans*, results in ectopic germline gene expression and the HTA phenotype (Petrella *et al.* 2011; Wang *et al.* 2005). We performed RNAi against the 15 TF HTA suppressors in a *lin-35* putative null mutant background to determine if the TFs found to suppress the HTA phenotype of *lin-54* mutants can do the same in *lin-35* mutants. RNAi against 11 of the 15 TF HTA suppressors genes in *lin-35* mutants showed significant suppression of HTA phenotype compared to empty vector RNAi (Figure 1c). Suppression of the HTA phenotype was generally weaker in *lin-35* mutants compared to *lin-54* mutants. Because lin-35 mutants have been shown to demonstrate enhanced somatic RNAi, we do not think these weaker phenotypes are due to a dampened RNAi effect (Ceron *et al.* 2007; Lehner *et al.* 2006; Wang *et al.* 2005; Wu *et al.* 2012). Instead the reduced HTA suppression in *lin-35* mutants may be in part due to the known pleiotropic effects of loss of *lin-35*, which generally shows slow growth and reduced fertility when compared to the *lin-54* mutant (Chi and Reinke 2006, Kudron *et al.* 2013, Rual *et al.* 2004; J.R.C. and L.N.P data not shown).

The HTA phenotype is a characteristic of not just DREAM complex mutants but also mutants in members of the HP1 complex (Petrella *et al.* 2011). LIN-13 is a member of the HP1 complex, which when mutated shows both ectopic expression of germline genes and the HTA phenotype (Coustham *et al.* 2006; Petrella *et al.* 2011). To determine if the loss of TF HTA suppressors suppresses the HTA phenotype when HP1 complex function is compromised, we performed RNAi against the 15 TF HTA suppressors in a *lin-13* mutant background. RNAi against all 15 TF HTA suppressors failed to significantly suppress the HTA phenotype in *lin-13* mutants (Figure 1c). DREAM complex bound loci overlap with only about one third of HPL complex bound loci (Garrigues *et al.* 2015; Goetsch *et al.* 2017; Rechtsteiner *et al.* 2019). This may lead to the misregulation of different subsets of genes in driving the HTA phenotype when each of the complexes is disrupted. Therefore, the loss of the TFs that suppress the HTA phenotype in DREAM complex mutants may not be sufficient to mitigate the

defects caused by loss of the HPL2 complex in *lin-13* mutants. Together, the combined results of *lin-54*, *lin-35*, and *lin-13* mutants suggest that TF HTA suppressors are acting to drive gene misexpression when the DREAM complex is compromised, but not when the HP1 complex is compromised.

A subset of TF HTA suppressors is required for PGL-1 misexpression in the soma of lin-54 mutants

P-granule proteins, which are exclusively expressed in the germline of wild-type, are ectopically expressed in the somatic cells of DREAM complex mutants (Wang *et al.* 2005; Petrella *et al.* 2011). To determine if TF HTA suppressors are necessary for the ectopic P-granule expression seen in DREAM complex mutants, we performed RNAi against the 15 TF HTA suppressors in a *lin-54* mutant background and measured the level of the P-granule protein PGL-1 the soma of L1 larvae at 26°. We determine the mean PGL-1 pixel intensity in the soma of each L1 animal normalized to the background (referred to as adjusted PGL-1 intensity) for a given RNAi treatment (Materials and methods). RNAi of nine of 15 TF HTA suppressors was able to significantly lower the adjusted PGL-1 intensity in *lin-54* mutants at 26° as compared to L4440 empty vector control (Figure 2 and Table 1). However, RNAi knockdown of each TF HTA suppressor, even those that significantly reduced the adjusted PGL-1 intensity, generally resulted in only a subset of the L1s in the population showing an adjusted PGL-1 intensity in the same range as is seen in wild-type worms. The incomplete penetrance seen with suppression of ectopic PGL-1 expression is similar to the partial suppression of the HTA phenotype, where a proportion of worms grow to the L4/Adult stage while others are arrested at the L1 stage. However, we did not see a correlation between those TFs that when knockeddown resulted in strong suppression of PGL-1 expression and those TFs that resulted in strong suppression of the HTA phenotype. Overall, only a subset of TF HTA suppressors appears to function in the ectopic expression of germline specific PGL-1.

In our control experiments, we observed that the adjusted PGL-1 intensity in somatic cells of *lin-54* mutants at 26° is significantly higher than the level in *lin-54* mutants at 20° (Figure S2). The adjusted PGL-1 intensity levels in the soma of *lin-54* mutants at 20° is not discernible from the wild type at either 20° or 26°, indicating the limitation of immunostaining in identifying potential subtle differences in adjusted PGL-1 intensity levels between wild type and *lin-54* mutants at 20° (Figure S2).

Wnt signaling modulates the HTA phenotype in lin-54 mutants

To determine if the TF HTA suppressors have related functional characteristics, we performed a functional enrichment analysis of the 15 TF candidates (Materials and Methods). Analysis using gProfiler g:GOSt functional profiling revealed overrepresentation of transcription factors involved in the Wnt signaling pathway (Table S3). Further analysis using PANTHER Overrepresentation Test, resulted in 53 over-represented Gene Ontology (GO) biological process terms (Table S4). The four most enriched GO terms were neuron fate specification, regulation of animal organ morphogenesis, regionalization, and positive regulation of transcription by RNA polymerase II. Neuronal fate decisions and regionalization are both known to be regulated by Wnt signaling (Bielen and Houart 2014; Mulligan and Cheyette 2017; Zwamborn *et al.* 2018). Additionally, five of the TF HTA suppressors, including LIN-11, MAB-5, LIN-11, VAB-3, and ZTF-6, have previously been shown to be associated with Wnt signaling (Doitsidou *et al.* 2018; Gupta and Sternberg 2002; Johnson and Chamberlin 2008, Maloof *et al.* 1999).
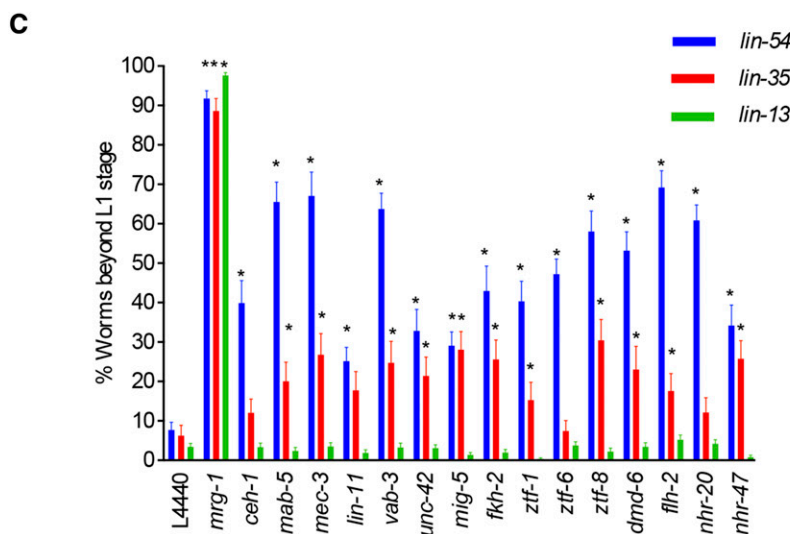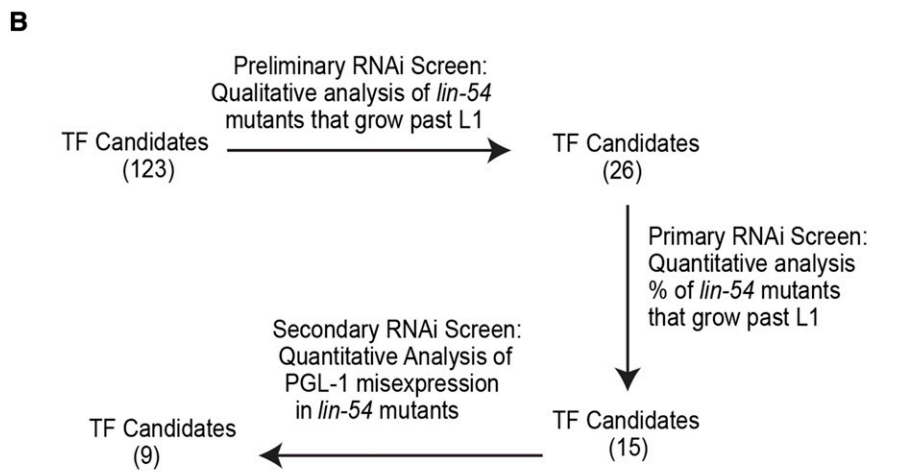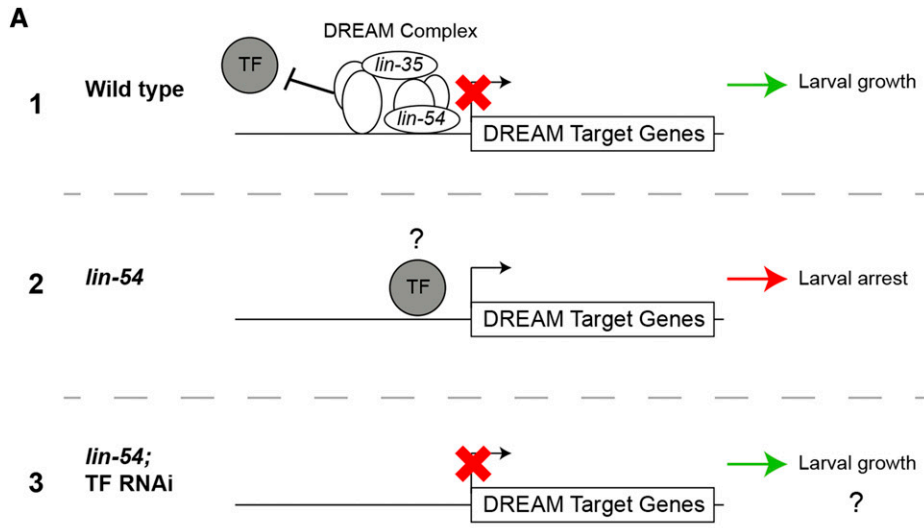
Figure 1 RNAi screen identifies 15 transcription factors that promote the HTA phenotype in DREAM complex mutants. (A) Model of DREAM complex target gene regulation (1) In the wild type, the DREAM complex represses germline gene misexpression in somatic cells and allows normal worm growth past the L1 stage at 26°C. (2) In *lin-54* mutants the DREAM complex cannot bind, which results in activation of DREAM target genes and the high temperature larval arrest (HTA) phenotype is observed at 26°C. We predict that under these conditions transcription factors bind (TF) to and activate DREAM target genes. (3) Therefore, when those TFs are knock-downed by RNAi in *lin-54* mutant background there should be a decrease in DREAM target gene expression and restored larval growth. (B) Workflow for RNAi screen to identify transcription factors involved in suppression of HTA phenotype and reduction in germline PGL-1 misexpression in somatic cells of *lin-54* mutants. (C) Knock-down of 15 and 11 transcription factors in *lin-54* and *lin-35* mutants respectively resulted in significant suppression of the HTA phenotype when compared to L4440 empty vector RNAi. There was no suppression of the HTA phenotype in *lin-13* mutants upon knock-down of any of the 15 transcription factors. RNAi against *mrg-1* was used as a positive control for HTA suppression. Significant percentage of growth to the L4/Adult stage compared to L4440 empty vector was determined by Fisher's Exact test (*P value ≤ 0.05). Error bars indicate standard error of proportion.

We were particularly interested in the possible role of Wnt signaling in DREAM complex mutant phenotypes, as previous data had shown an anterior-to-posterior (A-P) pattern to chromatin compaction defects in DREAM complex mutants (Costello and Petrella 2019). Wnt signaling is important in the establishment of the A-P axis during development and Wnt ligands are found in gradients along the A-P axis (Schroeder

RNAi Target	Transcription Factor Family[a]	No. of DREAM target promoters bound by TF[b]	HTA Suppression in lin-54	% Adult worms	Average of Adjusted PGL-1 intensity (SD)
WT	NA	NA	NA	97.97	2.16 (0.61)
L4440	NA	NA	NA	7.69	6.75 (1.60)
ceh-1	HD	14	Yes	39.9	4.37[c] (2.14)
mab-5	HD - HOX	3	Yes	65.53	6.68 (3.57)
mec-3	HD - LIM	3	Yes	67.12	4.48[c] (1.33)
lin-11	HD - LIM	7	Yes	25.13	6.09 (2.26)
vab-3	HD - PRD	13	Yes	63.73	5.79 (2.47)
unc-42	HD - PRD	14	Yes	32.8	4.02[c] (1.62)
mig-5	WH	24	Yes	29.05	3.08[c] (1.47)
fkh-2	WH - Fork Head	1	Yes	43.01	5.79[c] (3.26)
ztf-1	ZF - C2H2 - 4 fingers	12	Yes	40.36	3.87[c] (2.40)
ztf-6	ZF - C2H2 - 2 fingers	6	Yes	47.25	4.14 (2.31)
ztf-8	ZF - C2H2 - 3 fingers	12	Yes	58.04	5.69[c] (2.96)
dmd-6	ZF - DM	7	Yes	53.18	4.13[c] (2.19)
flh-2	ZF - FLYWCH	1	Yes	69.18	5.79 (1.854)
nhr-20	ZF - NHR	3	Yes	60.84	3.59[c] (1.38)
nhr-47	ZF - NHR	1	Yes	34.21	6.23 (1.57)

[a] Reece-Hoyes et al. 2011.
[b] Goetsch et al. 2017.
[c] Transcription factors with significantly lowered distribution of adjusted PGL-1 intensity when knocked-down in lin-54 mutants at 26°C compared to RNAi empty vector L4440.

and McGhee 1998). To assess if the Wnt signaling pathway plays a role in regulating the HTA phenotype, we performed RNAi against 41 known Wnt signaling associated genes (Sawa and Korswagen 2013) and scored for HTA suppression in a lin-54 mutant background (Figure 3a). RNAi against eight of the Wnt signaling genes resulted in embryonic lethality in both lin-54 and wildtype animals (Table S5). RNAi against an additional nine Wnt signaling genes resulted in embryonic lethality in only the lin-54 mutants (Table S5). This may be due to DREAM complex mutants being more sensitive than wild type to perturbations in Wnt signaling, or lin-54 mutants may have enhanced somatic RNAi similar other DREAM complex mutants (Ceron et al. 2007; Lehner et al. 2006; Wang et al. 2005; Wu et al. 2012). RNAi against 14 of the 24 remaining Wnt signaling genes significantly suppressed the HTA phenotype in lin-54 mutants (Figure 3b and Table S5). These genes encode products found at multiple levels of the Wnt signaling cascade, from Wnt ligands to cytoplasmic factors (Figure 3a).

Knockdown of three genes that function in Wnt ligand production and secretion, mom-1, vps-29, and snx-3, resulted in weak yet significant suppression of the HTA phenotype in lin-54 mutants (Figure 3b). Knock-down of two of four embryonically viable Wnt ligands, egl-20 and cwn-2, resulted in suppression of HTA (Figure 3b). EGL-20 is highly expressed in the posterior tail region in wild-type animals (Pan et al. 2006). Mis-expression of EGL-20 in lin-54 mutants could be associated with aberrant signaling leading to the HTA phenotype. However, we found that the EGL-20:GFP expression pattern in lin-54 mutants was limited to the posterior end of the L1 stage worm similar to the wild-type pattern at both 20° and 26° (Figure S3) (Whangbo and Kenyon 1999).

Among the transmembrane Wnt receptors tested, only RNAi against lin-18 suppressed the HTA phenotype to significant levels (Figure 3b). Two of the three canonical Frizzled GPCR receptors (lin-17 and mom-5) when knocked-down were embryonically lethal and therefore could not be tested (Table S5). LIN-18 and CAM-1 are tyrosine kinase receptors that are known to function in parallel to Frizzled GPCR receptors to regulate Wnt signaling (Inoue et al. 2004). Both the LIN-18 mammalian homolog (Ryk) and CAM-1 in C. elegans can signal through the Wnt planar cell polarity (PCP) pathway

through interactions with VANG-1 (Andre et al. 2012; Green et al. 2008). Interestingly, EGL-20 signals through CAM-1 and VANG-1 receptors in vulval precursor cells of C.elegans (Green et al. 2008). That only knock-down of lin-18 resulted suppression of HTA may reflect that the Wnt pathway utilized in the HTA phenotype is through non-frizzled receptors and the PCP pathway (see below).

RNAi against a number of genes encoding cytoplasmic transducers of the Wnt signal suppressed the HTA phenotype, including two Disheveled orthologs, mig-5 and dsh-1, and one Axin ortholog, pry-1 (Figure 3b). MOM-4 and TAP-1 are MAP kinase components that function to antagonize Wnt signaling by phosphorylation and inhibition of TCF, a Wnt downstream effector (Smit et al. 2004). We observed that knock-down of tap-1 suppressed the HTA phenotype. In lin-54 mutants, knock-down of mom-4 resulted in highly penetrant embryonic lethality. Only 2-4 larvae per experiment escaped passed embryonic stage, but all of those grew past L1 arrest stage. The small sample size did not permit significance testing (Figure 3b).

Interestingly, RNAi against all three non-canonical Wnt PCP genes, vang-1, fmi-1, and prkl-1, resulted in strong HTA suppression compared to L4440 empty vector RNAi (Figure 3b). This suggests a specific role for the non-canonical Wnt/PCP pathway in driving the HTA phenotype. Because RNAi against most of the downstream factors controlling Wnt pathway target gene expression were embryonically lethal, we could not assess their role in regulating the HTA phenotype (Table S4). Overall, a specific subset of Wnt signaling genes, found at multiple levels of the signaling cascade, showed suppression of the HTA phenotype.

The conserved Wnt/PCP component VANG-1 is required for the HTA phenotype, ectopic PGL-1 expression, and small brood size in lin-54 mutants

The strong suppression of the HTA phenotype in lin-54 mutants with the knock-down of any of the three Wnt PCP pathway components (vang-1, prkl-1, and fmi-1) led us to further investigate the genetic interaction of the DREAM complex and Wnt/PCP pathway. VANG-1 is the highly conserved C. elegans homolog of the

G3·Genes | Genomes | Genetics
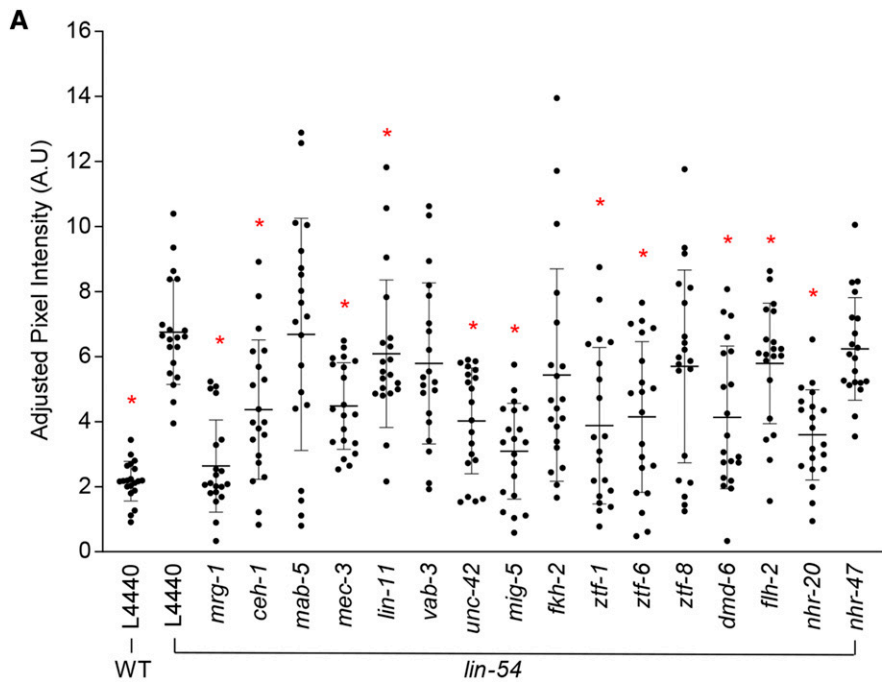
Figure 2 RNAi knock down of 9 transcription factor candidates in a *lin-54* mutant background at 26°C shows reduced ectopic PGL-1 expression. (A) Knock-down of 9 of 15 TF candidates tested showed a significant reduction in adjusted PGL-1 intensity somatic cells of *lin-54* mutants at 26°C when compared to *lin-54* mutants grown on L4440 empty vector bacteria. Y axis indicates the adjusted PGL-1 intensity. The dot plot shows the adjusted PGL-1 intensity for a population of L1s for a particular RNAi treatment. Kolmogorov-Smirnov test was done to compare empty vector L4440 in *lin-54* mutants with every TF. (*P value ≤ 0.05). The horizontal lines indicate the mean and SD of the distribution. (B) Representative images for the negative control (L4440 RNAi in a *lin-54* mutant background), positive controls (L4440 RNAi in WT, *mrg-1* RNAi in a *lin-54* mutant background) and a representative sample (*mig-5* RNAi in a *lin-54* mutant background). Arrows indicate primordial germ cells.
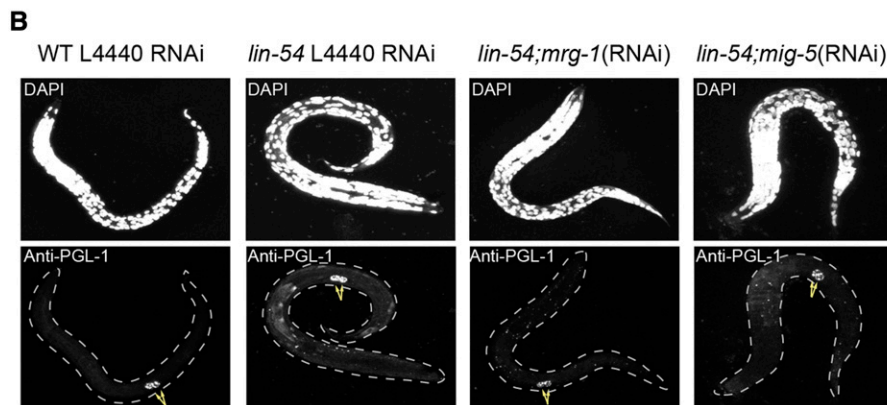
PCP pathway associated transmembrane Vangl protein and it is necessary for mediating PCP signaling (He *et al.* 2018; Honnen *et al.* 2012; Yang and Mlodzik 2015). We crossed *vang-1*(ok1142) mutation, which lack 162 amino acids of the C-terminus of VANG-1 (Honnen *et al.* 2012), with the lin-54(n2231) mutation to create a *lin-54*; *vang-1* double mutant. We found that the double mutant showed a complete suppression of the HTA phenotype (Figure 4a). Additionally, the adjusted PGL-1 intensity distribution in somatic cells of *lin-54*; *vang-1* mutants was significantly reduced in comparison to *lin-54* mutants at 26° (Figure 4b).

When analyzing the suppression of HTA, we observed that *lin-54*; *vang-1* double mutant worms at 26° were fertile. Mutations in most previously identified HTA suppressors, such as *mrg-1* and *mes-4*, result in sterility, (Fujita *et al.* 2002; Garvin *et al.* 1998, Petrella *et al.* 2011). We analyzed the brood size of hermaphrodites under three different temperature regimes: hermaphrodites kept at 20° continuously, hermaphrodites raised at 20° until the L4 stage that were then up-shifted to 26°, and hermaphrodites kept at 26° continuously. *lin-54* single mutants have significantly smaller mean brood sizes than wild type or *vang-1* single mutants at both 20° and when up-shifted to 26° (Figure 5). Due to the HTA phenotype, *lin-54* single mutants could not be analyzed

when raised at 26°. The smaller brood size seen in *lin-54* single mutants is completely suppressed in *lin-54*; *vang-1* double mutants. In fact, double mutants showed significantly larger mean brood sizes than wildtype hermaphrodites at all three temperatures tested (Figure 5). In summary, loss of *vang-1* produced almost complete suppression of the *lin-54* HTA phenotype, ectopic germline gene expression, and fertility defects.

DISCUSSION

Loss of the DREAM complex results in misexpression of germline genes in somatic cells and high temperature larval arrest (Petrella *et al.* 2011; Wang *et al.* 2005; Wu *et al.* 2012). Using an RNAi suppressor screen, we identified a set of 15 TFs that contribute to the HTA phenotype. Additionally, we found that genes that function in Wnt signaling, notably those in the Wnt/PCP pathway, are also required for the high temperature larval arrest. Based on these results, we propose a model whereby embryonic TFs and the Wnt/PCP pathway each contribute to ectopic activation of DREAM target genes, and the resulting larval arrest, in DREAM complex mutants.

The HTA phenotype of DREAM complex mutants has been attributed to significant gene misexpression in embryonic intestinal cells, leading to intestinal cell dysfunction and nutritional deprivation even in
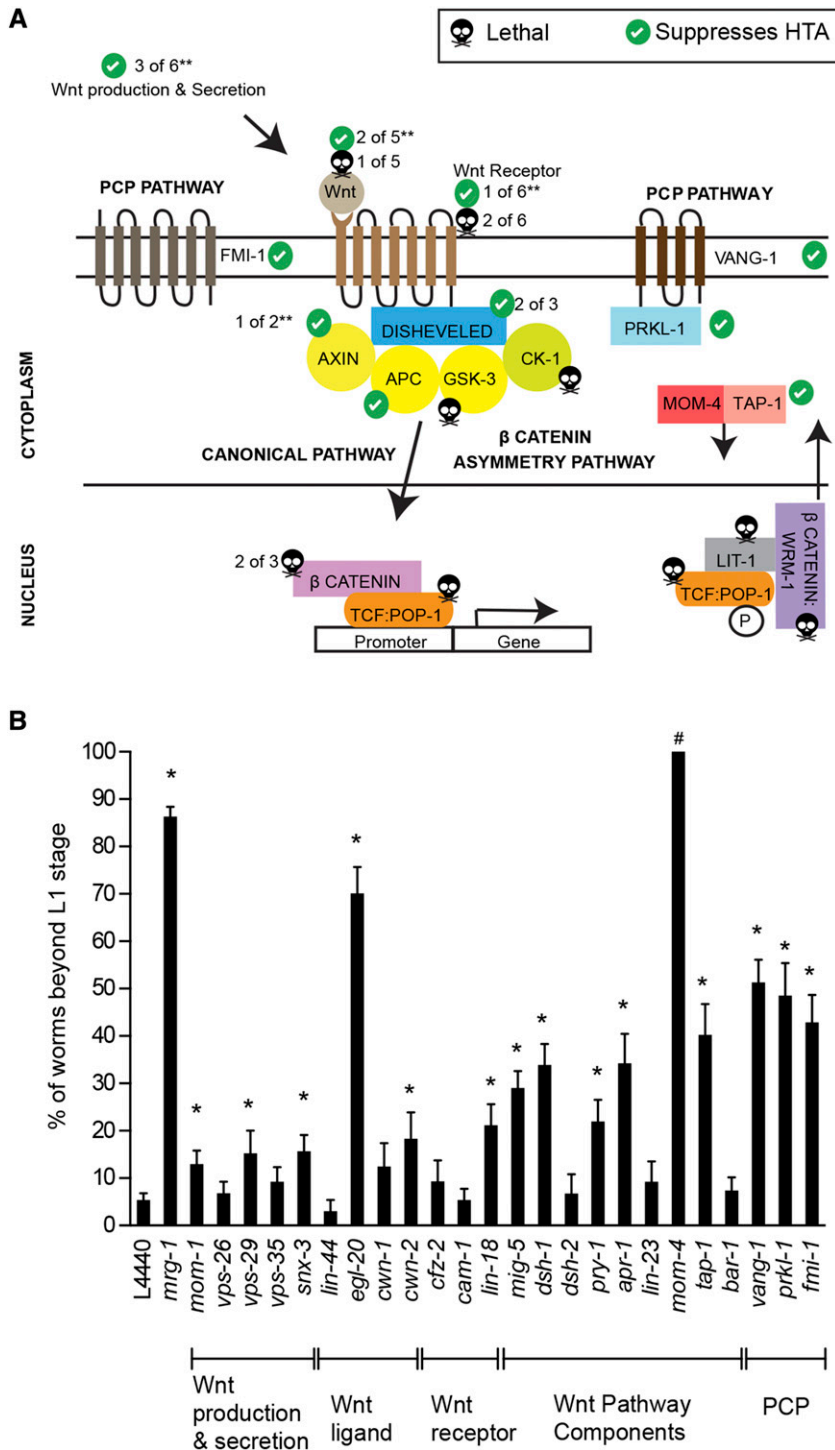
Figure 3 Fourteen Wnt signaling pathway components show HTA suppression phenotype in a *lin-54* mutants. (A) Schematic diagram of the Wnt signaling pathway in *C. elegans*. Check mark on a green filled circle and black skull with cross bone sign indicate genes that show suppression of HTA phenotype in *lin-54* mutants and embryonic lethality when knocked-down respectively. ** indicates that some genes were not tested (refer Table S5 for more details). (B) Knock-down of 14 of 41 Wnt pathway genes tested were able to suppress HTA phenotype in *lin-54* mutant background. Worms that had progeny after the knock-down of Wnt pathway genes in *lin-54* mutants are displayed in the graph. #RNAi of *mom-4* was almost completely embryonic lethal and gave rise to only 2-4 larvae per experiment, but all of those grew past L1 arrest stage. The number of worms scored for *mom-4* was too small a sample size to determine significance. Fisher's Exact Test was done to compare every Wnt gene RNAi with empty vector L4440. (*P value ≤0.05). Error bars indicate standard error of proportion.

the presence of food (Petrella *et al.* 2011). There are two potential sources for the TFs that we found contribute to gene expression in DREAM complex mutants. First, these TFs may be normally expressed in wild-type embryonic somatic tissues, but unable to bind DREAM targets in the presence of the DREAM complex. For this class of TFs, activation of DREAM target genes may result from their recruitment to novel gene targets in the absence of the DREAM complex. Second, the TFs themselves could be genes normally repressed by the DREAM complex, and are ectopically expressed in DREAM complex mutants. Analysis of single-cell RNA-seq data from the *C. elegans* embryo

showed that all but one of the TF HTA suppressors found in our screen are normally expressed in the wild-type embryonic intestinal lineage (Packer *et al.* 2019), a finding consistent with the former possibility. The sole exception is *ceh-1*, which is expressed embryonically only in the anal sphincter muscles, AVK neurons, and anterior body wall muscles but with no clear evidence of intestinal expression (Packer *et al.* 2019). Taken together, these data suggest that in the absence of the DREAM repressor complex, TFs normally expressed in embryonic somatic cells can be coopted to bind new genomic locations, leading to gene misexpression and cell fate changes.
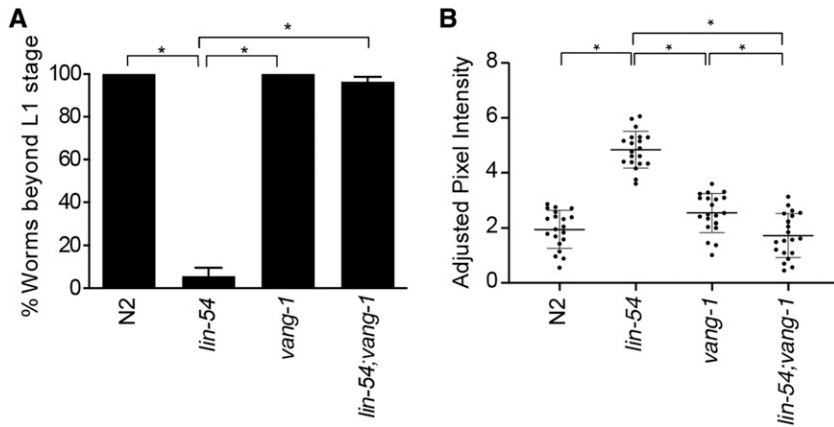
Figure 4 *lin-54*; *vang-1* mutants completely suppresses the HTA phenotype and show reduced ectopic PGL-1 expression close to wild-type levels. (A) Wild type, *vang-1* and *lin-54*; *vang-1* mutants do not show the HTA phenotype and grow to become adults in contrast to *lin-54* mutants that arrested at the L1 stage at 26°C. (Fisher's Exact test *P value ≤ 0.05). Error bars indicate standard error of proportion. (B) *lin-54*; *vang-1* mutants show reduced somatic adjusted PGL-1 intensity at 26°C comparable to wild-type levels. Y-axis indicates adjusted PGL-1 intensity. The dot plot shows the adjusted PGL-1 intensity for a population of L1s under a particular RNAi treatment. The horizontal lines indicate the mean and SD of the distribution. (Kolmogorov-Smirnov test *P value ≤ 0.05).

We found that only a subset of TF HTA suppressors was necessary for ectopic expression of PGL-1 in *lin-54* mutants. That the HTA phenotype may be correlated with the ectopic germline gene expression in DREAM complex mutants was proposed based on two pieces of data. First, the significant number of germline genes that are ectopically expressed in DREAM complex mutants suggested a level of fate conversion that could lead to the intestinal dysfunction that underlies the HTA phenotype. Second, knock-down of chromatin factors that promote germline fate results in both strong suppression ectopic germline expression and the HTA phenotype (Petrella *et al.* 2011). However, we did not see strong correlation between the level of suppression of ectopic PGL-1 expression and the HTA phenotype. This may indicate that there is little correlation between general ectopic germline gene expression and the intestinal dysfunction leading to the HTA phenotype. However, it may be that PGL-1 expression is not an accurate reflection of the change in broader germline gene expression when TF HTA suppressors are knocked-down. Analysis of changes in DREAM targets genome-wide when the HTA phenotype is suppressed will be necessary to more completely determine if there is correlation between these two phenotypes.

In our RNAi screen, we tested all TFs that were capable of binding to DREAM complex target genes in a Y1 Hybrid assay (Reece-Hoyes *et al.* 2011). While these proteins are predicted to function as transcription factors based on the presence of known DNA binding domains, they have not necessarily been validated as TFs *in vivo*. In the Y1 hybrid data set, MIG-5 bound 50% of the DREAM target genes that were tested, the largest number of all the TF HTA suppressors (Table 1). Knockdown of *mig-5* showed strong suppression of the HTA phenotype and ectopic PGL-1 expression. However, MIG-5 is not a known transcription factor, but instead one of three worm Disheveled (Dsh) proteins, which all contain a winged-helix DNA binding domain. Dsh proteins function in Wnt signaling by stabilizing activated β-catenin in the cytoplasm (Figure 3a) (Jackson and Eisenmann 2012; Salic *et al.* 2000). Dsh proteins are also known to be an important branch point between the canonical Wnt and Wnt/PCP pathways (Yan *et al.* 2001; Salic *et al.* 2000; Wallingford and Habas 2005). In some organisms Dsh proteins shuttle to the nucleus, which is has been shown to be necessary for Wnt signaling (Cheyette *et al.* 2002; Habas and Dawid 2005; Itoh *et al.* 2005; Torres and Nelson 2000; Weitzman 2005). Furthermore, in mammals Dsh proteins have been shown to interact directly with transcription factors within the nucleus (Gan *et al.* 2008; Wang *et al.* 2015). Nuclear localization of MIG-5 has not been observed in *C. elegans*; however, the known nuclear localization signal of *Xenopus* Dsh is almost completely conserved within MIG-5 (Itoh *et al.* 2005). Further analysis is needed to determine if we have uncovered a novel role for MIG-5 in the nucleus in *C. elegans* or if MIG-5 is solely acting by transducing non-canonical Wnt/PCP signaling in DREAM complex mutants.

One of the striking findings from our screens is the substantial role that Wnt/PCP signaling plays in driving the HTA and germline gene expression phenotypes in *lin-54* mutants. Many components of the Wnt signaling cascade can differ between tissues and developmental times, which in turn can lead to different outcomes depending on the specific cellular context (Eisenmann 2005; Hardin and King 2008; Kwon *et al.* 2008; Sokol 2015). Therefore, it is unclear if the suppression of the HTA phenotype seen with loss of other Wnt signaling components is due to the specific loss of canonical Wnt signaling or Wnt/PCP signaling. However, our data supports an important role for Wnt/PCP signaling in the HTA phenotype. First, loss of any of the three components specific to the Wnt/PCP pathway, *vang-1*, *prkl-1*, and *fmi-1*, all lead to significant suppression of HTA. Second, some of the other Wnt signaling components that suppress the HTA phenotype have been shown to interact with the Wnt/PCP pathway. Most strikingly is the significant suppression seen with knockdown of the Wnt ligand *egl-20*.
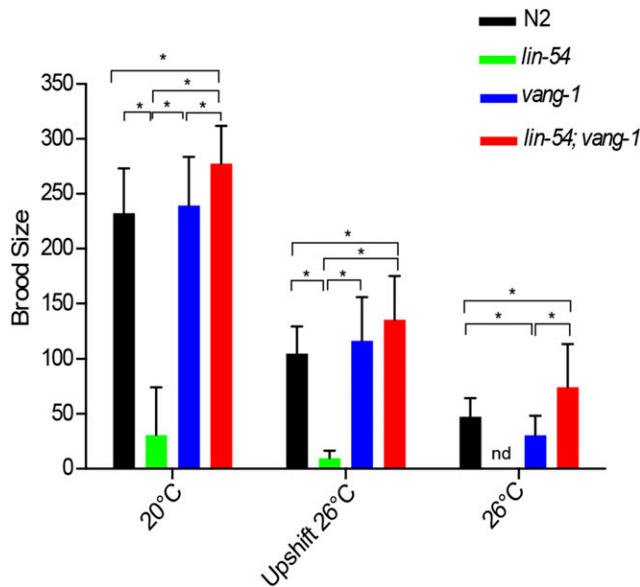
Figure 5 *lin-54*; *vang-1* mutants suppresses small brood size phenotype of *lin-54* mutants. The *lin-54*; *vang-1* mutant showed a significantly larger brood size compared to wild type, *lin-54*, and *vang-1* mutants at 20°C and 26°C. (Welch's T test *P value ≤ 0.05). Error bars indicate standard deviation.

Of the five Wnt ligands, EGL-20 has most often been shown to interact with the Wnt/PCP pathway (Green *et al.* 2008; Mentink *et al.* 2018). In the intestine, the only documented role of Wnt/PCP signaling is for proper orientation of intestinal cells during intestinal morphogenesis (Asan *et al.* 2016; Hoffmann *et al.* 2010), but in other tissues Wnt/PCP signaling can help to regulate A-P fate specification (Ackley 2014; Antic *et al.* 2010; He *et al.* 2018; Mattes *et al.* 2018; Mentink *et al.* 2018). It is still unclear what role Wnt/PCP signaling plays in regulating gene expression and fate specification in the intestine.

How could the Wnt/PCP pathway be driving the HTA phenotype? We propose two non-mutually exclusive models of how Wnt/PCP signaling could drive ectopic DREAM complex target expression leading to HTA. The first model is that Wnt/PCP signaling may be necessary for the expression of the transcription factors that directly bind to DREAM target loci and drive their ectopic expression. The proper asymmetric anterior-posterior (A-P) expression of three of the TF HTA suppressors found in our screen, MAB-5, LIN-11, and VAB-3, requires Wnt signaling in neuronal and vulval tissues (Gupta and Sternberg 2002; Johnson and Chamberlin 2008, Maloof *et al.* 1999). A fourth TF HTA suppressor, MEC-3, also has known asymmetric A-P expression, although this pattern has yet to be attributed specifically to Wnt signaling (Way *et al.* 1992). The second model is that Wnt/PCP signaling regulates the A-P patterning of the intestine, and that this pattern is itself a necessary state for ectopic expression of DREAM target loci. While chromatin structure in wild-type embryonic cells undergoes rapid compaction, we previously showed that this process is delayed in DREAM complex mutants, and shows an A-P pattern where anterior cells are more severely delayed (Costello and Petrella 2019). One of the major pathways that helps to establish A-P axis patterning in *C. elegans* is Wnt signaling (Lin *et al.* 1998; Schroeder and McGhee 1998). Therefore, underlying aspects of a A-P pattern established by Wnt signaling may facilitate the delayed chromatin compaction in DREAM complex mutants at 26°, which in turn allows TFs to bind and activate germline genes. Distinguishing between these two models will require further analysis of the interaction of Wnt signaling, chromatin compaction, and TF expression in DREAM complex mutants.

The DREAM complex, ectopic expression of germline genes, and Wnt/PCP signaling all have known roles in cancer acquisition and progression. The DREAM complex is completely conserved in mammals, and loss of DREAM complex function is associated with cancers (Engeland 2018; Patel *et al.* 2019; Reichert *et al.* 2010). Some tumors are known to ectopically express a group of germline specific genes called cancer-testis (CT) genes. CT gene expression has been shown to correlate with increased proliferative index, higher tumor grade, and poorer response to therapies in many studies and across a broad range of tumor types (Gure *et al.* 2005; Wang *et al.* 2016; Whitehurst 2014; Xu *et al.* 2015; Yakirevich *et al.* 2003). Wnt/PCP signaling is important in cancer progression and metastasis in a number of tumor types including lung cancer, melanoma, and breast cancer (Humphries and Mlodzik 2018; Katoh 2005). Our data indicate that these three pathways are linked in *C. elegans* where Wnt signaling via the non-canonical PCP mechanism leads to activation of germline genes in the absence of DREAM complex binding. The identification of the upstream VANG-1 of Wnt/PCP pathway provides a useful starting point to help dissect out the intermediate signaling molecules to activate germline genes in somatic cells of DREAM complex mutants. Our findings provide insight into potential pathways that are important in the activation of germline genes in cancer cells that could be targets to limit cancer progression.

LITERATURE CITED

Ackley, B. D., 2014 Wnt signaling and planar cell polarity genes regulate axon guidance along the anteroposterior axis in C. elegans. Dev. Neurobiol. 74: 781–796. https://doi.org/10.1002/dneu.22146

Andre, P., Q. Wang, N. Wang, B. Gao, A. Schilit *et al.*, 2012 The Wnt Coreceptor Ryk Regulates Wnt/Planar Cell Polarity by Modulating the Degradation of the Core Planar Cell Polarity Component Vangl2. J. Biol. Chem. 287: 44518–44525. https://doi.org/10.1074/jbc.M112.414441

Antic, D., J. L. Stubbs, K. Suyama, C. Kintner, M. P. Scott *et al.*, 2010 Planar cell polarity enables posterior localization of nodal cilia and left-right axis determination during mouse and Xenopus embryogenesis. PLoS One 5: e8999. https://doi.org/10.1371/journal.pone.0008999

Asan, A., S. A. Raiders, and J. R. Priess, 2016 Morphogenesis of the C. elegans Intestine Involves Axon Guidance Genes. PLoS Genet. 12: e1005950 (erratum: PLOS Genetics 12: e1006077). https://doi.org/10.1371/journal.pgen.1005950

Ashburner, M., C. A. Ball, J. A. Blake, D. Botstein, H. Butler *et al.*, 2000 Gene Ontology: tool for the unification of biology. Nat. Genet. 25: 25–29. https://doi.org/10.1038/75556

Bielen, H., and C. Houart, 2014 The Wnt cries many: Wnt regulation of neurogenesis through tissue patterning, proliferation, and asymmetric cell division. Dev. Neurobiol. 74: 772–780. https://doi.org/10.1002/dneu.22168

Brenner, S., 1974 The genetics of *Caenorhabditis elegans*. Genetics 77: 71–94.

Ceron, J., J. F. Rual, A. Chandra, D. Dupuy, M. Vidal *et al.*, 2007 Large-scale RNAi screens identify novel genes that interact with the C. elegans retinoblastoma pathway as well as splicing-related components with synMuv B activity. BMC Dev. Biol. 7: 30. https://doi.org/10.1186/1471-213X-7-30

Chang, Y., X. Wang, Y. Xu, L. Yang, Q. Qian *et al.*, 2019 Comprehensive characterization of cancer-testis genes in testicular germ cell tumor. Cancer Med-us 8: 3511–3519. https://doi.org/10.1002/cam4.2223

Cheyette, B. N., J. S. Waxman, J. R. Miller, K.-I. Takemaru, L. C. Sheldahl *et al.*, 2002 Dapper, a Dishevelled-Associated Antagonist of β-Catenin and JNK Signaling, Is Required for Notochord Formation. Dev. Cell 2: 449–461. https://doi.org/10.1016/S1534-5807(02)00140-5

Chi, W., and V. Reinke, 2006 Promotion of oogenesis and embryogenesis in the C. elegans gonad by EFL-1/DPL-1 (E2F) does not require LIN-35 (pRB). Development 133: 3147–3157 (erratum: Development 133: 3495). https://doi.org/10.1242/dev.02490

Costello, M. E., and L. N. Petrella, 2019 C. elegans synMuv B proteins regulate spatial and temporal chromatin compaction during development. Development 146: dev.174383.

Coustham, V., C. Bedet, K. Monier, S. Schott, M. Karali *et al.*, 2006 The C. elegans HP1 homologue HPL-2 and the LIN-13 zinc finger protein form a complex implicated in vulval development. Dev. Biol. 297: 308–322. https://doi.org/10.1016/j.ydbio.2006.04.474

Cui, M., B. E. Kim, and M. Han, 2006 Diverse Chromatin Remodeling Genes Antagonize the Rb-Involved SynMuv Pathways in C. elegans. PLoS Genet. 2: e74. https://doi.org/10.1371/journal.pgen.0020074

Doitsidou, M., G. Minevich, J. R. Kroll, G. Soete, S. Gowtham *et al.*, 2018 A *Caenorhabditis elegans* zinc finger transcription factor, *ztf-6*, required for specification of a dopamine neuron-production lineage. G3 (Bethesda) 8: 17–26. https://doi.org/10.1534/g3.117.300132

Engeland, K., 2018 Cell cycle arrest through indirect transcriptional repression by p53: I have a DREAM. Cell Death Differ. 25: 114–132. https://doi.org/10.1038/cdd.2017.172

Eisenmann, D. M., 2005 Wnt signaling. (June 25, 2005), WormBook, ed. The C. elegans Research Community WormBook, http://www.wormbook.org, https://doi.org/10.1895/wormbook.1.7.1

Fujita, M., T. Takasaki, N. Nakajima, T. Kawano, Y. Shimura *et al.*, 2002 MRG-1, a mortality factor-related chromodomain protein, is required maternally for primordial germ cells to initiate mitotic proliferation in C. elegans. Mech. Dev. 114: 61–69. https://doi.org/10.1016/S0925-4773(02)00058-8

Fuxman Bass, J. I., C. Pons, L. Kozlowski, J. S. Reece-Hoyes, S. Shrestha *et al.*, 2016 A gene-centered C. elegans protein-DNA interaction network provides a framework for functional predictions. Mol. Syst. Biol. 12: 884–884. https://doi.org/10.15252/msb.20167131

Gan, X., J. Wang, Y. Xi, Z. Wu, Y. Li *et al.*, 2008 Nuclear Dvl, c-Jun, beta-catenin, and TCF form a complex leading to stabilization of beta-catenin-TCF interaction. J. Cell Biol. 180: 1087–1100. https://doi.org/10.1083/jcb.200710050

Garrigues, J. M., S. Sidoli, B. A. Garcia, and S. Strome, 2015 Defining heterochromatin in C. elegans through genome-wide analysis of the heterochromatin protein 1 homolog HPL-2. Genome Res. 25: 76–88. https://doi.org/10.1101/gr.180489.114

Garvin, C., R. Holdeman, and S. Strome, 1998 The phenotype of mes-2, mes-3, mes-4 and mes-6, maternal-effect genes required for survival of the germline in Caenorhabditis elegans, is sensitive to chromosome dosage. Genetics 148: 167–185.

Goetsch, P. D., J. M. Garrigues, and S. Strome, 2017 Loss of the Caenorhabditis elegans pocket protein LIN-35 reveals MuvB's innate function as the repressor of DREAM target genes. PLoS Genet. 13: e1007088. https://doi.org/10.1371/journal.pgen.1007088

Green, J. L., T. Inoue, and P. W. Sternberg, 2008 Opposing Wnt pathways orient cell polarity during organogenesis. Cell 134: 646–656. https://doi.org/10.1016/j.cell.2008.06.026

Gross, K., A. Wronski, A. Skibinski, S. Phillips, and C. Kuperwasser, 2016 Cell Fate Decisions During Breast Cancer Development. J. Dev. Biol. 4: 4. https://doi.org/10.3390/jdb4010004

Gure, A. O., R. Chua, B. Williamson, M. Gonen, C. A. Ferrera *et al.*, 2005 Cancer-Testis Genes Are Coordinately Expressed and Are Markers of Poor Outcome in Non–Small Cell Lung Cancer. Clin. Cancer Res. 11: 8055–8062. https://doi.org/10.1158/1078-0432.CCR-05-1203

Gupta, B. P., and P. W. Sternberg, 2002 Tissue-specific regulation of the LIM homeobox gene *lin-11* during development of the *Caenorhabditis elegans* egg-laying system. Dev. Biol. 247: 102–115. https://doi.org/10.1006/dbio.2002.0688

Habas, R., and I. B. Dawid, 2005 Dishevelled and Wnt signaling: is the nucleus the final frontier? J. Biol. 4: 2. https://doi.org/10.1186/jbiol22

Hardin, J., and R. S. King, 2008 The long and the short of Wnt signaling in C. elegans. Curr. Opin. Genet. Dev. 18: 362–367. https://doi.org/10.1016/j.gde.2008.06.006

Harrison, M., C. Ceol, X. Lu, and H. Horvitz, 2006 Some C. elegans class B synthetic multivulva proteins encode a conserved LIN-35 Rb-containing complex distinct from a NuRD-like complex. Proc. Natl. Acad. Sci. USA 103: 16782–16787. https://doi.org/10.1073/pnas.0608461103

He, C. W., C. P. Liao, C.-K. Chen, J. Teulière, C.-H. Chen *et al.*, 2018 The polarity protein VANG-1 antagonizes Wnt signaling by facilitating Frizzled endocytosis. Development 145: dev168666. https://doi.org/10.1242/dev.168666

Heinz, S., and C. K. Glass, 2012 Roles of Lineage-Determining Transcription Factors in Establishing Open Chromatin: Lessons From High-Throughput Studies. Curr Top Microbiol 356: 1–15. https://doi.org/10.1007/82_2011_142

Hernández-Arriaga, A. M., T. S. Rubio-Lepe, M. Espinosa, and G. del Solar, 2009 Repressor CopG prevents access of RNA polymerase to promoter and actively dissociates open complexes. Nucleic Acids Res. 37: 4799–4811. https://doi.org/10.1093/nar/gkp503

Hoffmann, M., C. Segbert, G. Helbig, and O. Bossinger, 2010 Intestinal tube formation in Caenorhabditis elegans requires vang-1 and egl-15 signaling. Dev. Biol. 339: 268–279. https://doi.org/10.1016/j.ydbio.2009.12.002

Honnen, S. J., C. Büchter, V. Schröder, M. Hoffmann, Y. Kohara *et al.*, 2012 C. elegans VANG-1 Modulates Life Span via Insulin/IGF-1-Like Signaling. PLoS One 7: e32183. https://doi.org/10.1371/journal.pone.0032183

Humphries, A. C., and M. Mlodzik, 2018 From instruction to output: Wnt/PCP signaling in development and cancer. Curr. Opin. Cell Biol. 51: 110–116. https://doi.org/10.1016/j.ceb.2017.12.005

Inoue, T., H. S. Oz, D. Wiland, S. Gharib, R. Deshpande *et al.*, 2004 C. elegans LIN-18 is a Ryk ortholog and functions in parallel to LIN-17/Frizzled in Wnt signaling. Cell 118: 795–806. https://doi.org/10.1016/j.cell.2004.09.001

Itoh, K., B. K. Brott, G. U. Bae, M. J. Ratcliffe, and S. Y. Sokol, 2005 Nuclear localization is required for Dishevelled function in Wnt/β-cetenin signaling. J. Biol. 4: 3. https://doi.org/10.1186/jbiol20

Jackson, B. M., and D. M. Eisenmann, 2012 β-Catenin-Dependent Wnt Signaling in C. elegans: Teaching an Old Dog a New Trick. Csh Perspect Biol 4: a007948. https://doi.org/10.1101/cshperspect.a007948

Johnson, R. W., and H. M. Chamberlin, 2008 Positive and negative regulatory inputs restrict *pax-6/vab-3* transcription to sensory organ precursors in *Caenorhabditis elegans*. Mech. Dev. 125: 486–497. https://doi.org/10.1016/j.mod.2008.01.007

Katoh, M., 2005 Wnt/PCP signaling pathway and human cancer. Oncol. Rep. 14: 1583–1588.

Kawasaki, I., Y.-H. Shim, J. Kirchner, J. Kaminker, W. B. Wood *et al.*, 1998 PGL-1, a Predicted RNA-Binding Component of Germ Granules, Is Essential for Fertility in C. elegans. Cell 94: 635–645. https://doi.org/10.1016/S0092-8674(00)81605-0

Kudron, M., W. Niu, Z. Lu, G. Wang, M. Gerstein *et al.*, 2013 Tissue-specific direct targets of Caenorhabditis elegans Rb/E2F dictate distinct somatic and germline programs. Genome Biol. 14: R5. https://doi.org/10.1186/gb-2013-14-1-r5

Kwon, C., K. R. Cordes, and D. Srivastava 2008 Wnt/beta-catenin signaling acts at multiple developmental stages to promote mammalian cardiogenesis. Cell Cycle 7: 3815–3818. https://doi.org/10.4161/cc.7.24.7189

Latorre, I., M. A. Chesney, J. M. Garrigues, P. Stempor, A. Appert *et al.*, 2015 The DREAM complex promotes gene body H2A.Z for target repression. Genes Dev. 29: 495–500. https://doi.org/10.1101/gad.255810.114

Lehner, B., A. Calixto, C. Crombie, J. Tischler, A. Fortunato *et al.*, 2006 Loss of LIN-35, the Caenorhabditis elegans ortholog of the tumor suppressor p105Rb, results in enhanced RNA interference. Genome Biol. 7: R4. https://doi.org/10.1186/gb-2006-7-1-r4

Li, P., and W. J. Leonard, 2018 Chromatin Accessibility and Interactions in the Transcriptional Regulation of T Cells. Front. Immunol. 9: 2738. https://doi.org/10.3389/fimmu.2018.02738

Lin, R., R. Hill, and J. Priess, 1998 POP-1 and anterior-posterior fate decisions in C. elegans embryos. Cell 92: 229–239. https://doi.org/10.1016/S0092-8674(00)80917-4

Maloof, J. N., J. Whangbo, J. M. Harris, G. D. Jongeward, and C. Kenyon, 1999 A Wnt signaling pathway controls hox gene expression and neuroblast migration in *C. elegans*. Development 126: 37–49.

Mattes, B., Y. Dang, G. Greicius, L. Kaufmann, B. Prunsche *et al.*, 2018 Wnt/PCP controls spreading of Wnt/β-catenin signals by cytonemes in vertebrates. eLife 7. https://doi.org/10.7554/eLife.36953

Mentink, R. A., L. Rella, T. W. Radaszkiewicz, T. Gybel, M. C. Betist *et al.*, 2018 The planar cell polarity protein VANG-1/Vangl negatively regulates Wnt/β-catenin signaling through a Dvl dependent mechanism. PLoS Genet. 14: e1007840. https://doi.org/10.1371/journal.pgen.1007840

Mi, H., A. Muruganujan, D. Ebert, X. Huang, and P. D. Thomas, 2019 PANTHER version 14: more genomes, a new PANTHER GO-slim and improvements in enrichment analysis tools. Nucleic Acids Res. 47: D419–D426. https://doi.org/10.1093/nar/gky1038

Mulligan, K. A., and B. N. Cheyette, 2017 Neurodevelopmental Perspectives on Wnt Signaling in Psychiatry. Mol. Neuropsychiatry 2: 219–246. https://doi.org/10.1159/000453266

Mutlu, B., H.-M. Chen, D. H. Hall, and S. E. Mango, 2018 MET-2, a SETDB1 family methyltransferase, coordinates embryo events through distinct histone H3 methylation states. bioRxiv. https://doi.org/doi:10.1101/429902

Packer, J. S., Q. Zhu, C. Huynh, P. Sivaramakrishnan, E. Preston *et al.*, 2019 A lineage-resolved molecular atlas of C. elegans embryogenesis at single-cell resolution. Science 365: eaax1971.

Pan, C.-L., J. Howell, S. G. Clark, M. Hilliard, S. Cordes *et al.*, 2006   Multiple Wnts and Frizzled Receptors Regulate Anteriorly Directed Cell and Growth Cone Migrations in Caenorhabditis elegans. Dev. Cell 10: 367–377. https://doi.org/10.1016/j.devcel.2006.02.010

Patel, A. J., Y. W. Wan, R. Al-Ouran, J. P. Revelli, M. F. Cardenas *et al.*, 2019   Molecular profiling predicts meningioma recurrence and reveals loss of DREAM complex repression in aggressive tumors. Proc. Natl. Acad. Sci. USA 116: 21715–21726. https://doi.org/10.1073/pnas.1912858116

Petrella, L. N., W. Wang, C. A. Spike, A. Rechtsteiner, V. Reinke *et al.*, 2011   synMuv B proteins antagonize germline fate in the intestine and ensure C. elegans survival. Development 138: 1069–1079. https://doi.org/10.1242/dev.059501

Pitt, J. N., J. Schisa, and J. Priess, 2000   P Granules in the Germ Cells of Caenorhabditis elegans Adults Are Associated with Clusters of Nuclear Pores and Contain RNA. Dev. Biol. 219: 315–333. https://doi.org/10.1006/dbio.2000.9607

Praggastis, S. A., and C. S. Thummel, 2017   Right time, right place: the temporal regulation of developmental gene expression. Genes Dev. 31: 847–848. https://doi.org/10.1101/gad.301002.117

Raudvere, U., L. Kolberg, I. Kuzmin, T. Arak, P. Adler *et al.*, 2019   g: Profiler: a web server for functional enrichment analysis and conversions of gene lists (2019 update). Nucleic Acids Res. 47: W191–W198. https://doi.org/10.1093/nar/gkz369

Rechtsteiner, A., M. E. Costello, T. A. Egelhofer, J. M. Garrigues, S. Strome *et al.*, 2019   Repression of Germline Genes in *Caenorhabditis elegans* Somatic Tissues by H3K9 Dimethylation of Their Promoters. Genetics 212: 125–140. https://doi.org/10.1534/genetics.118.301878

Reece-Hoyes, J. S., A. Diallo, B. Lajoie, A. Kent *et al.*, 2011   Enhanced yeast one-hybrid assays for high-throughput gene-centered regulatory network mapping. Nat. Methods 8: 1059–1064. https://doi.org/10.1038/nmeth.1748

Reichert, N., S. Wurster, T. Ulrich, K. Schmitt, S. Hauser *et al.*, 2010   Lin9, a Subunit of the Mammalian DREAM Complex, Is Essential for Embryonic Development, for Survival of Adult Mice, and for Tumor Suppression. Mol. Cell. Biol. 30: 2896–2908. https://doi.org/10.1128/MCB.00028-10

Rual, J.-F., J. Ceron, J. Koreth, T. Hao, A.-S. Nicot *et al.*, 2004   Toward improving Caenorhabditis elegans phenome mapping with an ORFeome-based RNAi library. Genome Res. 14: 2162–2168. https://doi.org/10.1101/gr.2505604

Sadasivam, S., and J. A. DeCaprio, 2013   The DREAM complex: master coordinator of cell cycle-dependent gene expression. Nat. Rev. Cancer 13: 585–595 (erratum: Nat. Rev. Cancer 13:585). https://doi.org/10.1038/nrc3556

Salic, A., E. Lee, L. Mayer, and M. W. Kirschner, 2000   Control of beta-Catenin Stability: Reconstitution of the Cytoplasmic Steps of the Wnt Pathway in Xenopus Egg Extracts. Mol. Cell 5: 523–532. https://doi.org/10.1016/S1097-2765(00)80446-3

Sawa, H., and H. C. Korswagen, 2013   Wnt signaling in C. elegans. (December 9, 2013), Wormbook, ed. The C. elegans Research Community Workbook, http://www.wormbook.org

Schroeder, D. F., and J. D. McGhee, 1998   Anterior-posterior patterning within the Caenorhabditis elegans endoderm. Development 125: 4877.

Smit, L., A. Baas, J. Kuipers, H. Korswagen, M. van de Wetering *et al.*, 2004   Wnt activates the Tak1/Nemo-like kinase pathway. J. Biol. Chem. 279: 17232–17240. https://doi.org/10.1074/jbc.M307801200

Smith, J., A. Zyoud, and C. Allegrucci, 2019   A Case of Identity: HOX Genes in Normal and Cancer Stem Cells. Cancers (Basel) 11: 512. https://doi.org/10.3390/cancers11040512

Sokol, S. Y., 2015   Spatial and temporal aspects of Wnt signaling and planar cell polarity during vertebrate embryonic development. Semin. Cell Dev. Biol. 42: 78–85. https://doi.org/10.1016/j.semcdb.2015.05.002

Strome, S., and W. B. Wood, 1983   Generation of asymmetry and segregation of germ-line granules in early C. elegans embryos. Cell 35: 15–25. https://doi.org/10.1016/0092-8674(83)90203-9

Tabuchi, T. M., B. Deplancke, N. Osato, L. J. Zhu, I. M. Barrasa *et al.*, 2011   Chromosome-Biased Binding and Gene Regulation by the Caenorhabditis elegans DRM Complex. PLoS Genet. 7: e1002074. https://doi.org/10.1371/journal.pgen.1002074

Torres, M., and W. Nelson, 2000   Colocalization and redistribution of dishevelled and actin during Wnt-induced mesenchymal morphogenesis. J. Cell Biol. 149: 1433–1442. https://doi.org/10.1083/jcb.149.7.1433

Unhavaithaya, Y., T. Shin, N. Miliaras, J. Lee, T. Oyama *et al.*, 2002   MEP-1 and a homolog of the NURD complex component Mi-2 act together to maintain germline-soma distinctions in C. elegans. Cell 111: 991–1002. https://doi.org/10.1016/S0092-8674(02)01202-3

Wallingford, J. B., and R. Habas, 2005   The developmental biology of Dishevelled: an enigmatic protein governing cell fate and cell polarity. Development 132: 4421–4436. https://doi.org/10.1242/dev.02068

Wang, C., Y. Gu, K. Zhang, K. Xie, M. Zhu *et al.*, 2016   Systematic identification of genes with a cancer-testis expression pattern in 19 cancer types. Nat. Commun. 7: 10499. https://doi.org/10.1038/ncomms10499

Wang, D., S. Kennedy, D. Conte, J. K. Kim, H. W. Gabel *et al.*, 2005   Somatic misexpression of germline P granules and enhanced RNA interference in retinoblastoma pathway mutants. Nature 436: 593–597. https://doi.org/10.1038/nature04010

Wang, W., X. Li, M. Lee, S. Jun, K. E. Aziz *et al.*, 2015   FOXKs promote Wnt/β-catenin signaling by translocating DVL into the nucleus. Dev. Cell 32: 707–718. https://doi.org/10.1016/j.devcel.2015.01.031

Way, J. C., J. Q. Run, and A. Y. Wang, 1992   Regulation of anterior cell-specific *mec-3* expression during asymmetric cell division in C. elegans. Dev. Dyn. 194: 289–302. https://doi.org/10.1002/aja.1001940405

Weitzman, J. B., 2005   Dishevelled nuclear shuttling. J. Biol. 4: 1. https://doi.org/10.1186/jbiol21

Whangbo, J., and C. Kenyon, 1999   A Wnt Signaling System that Specifies Two Patterns of Cell Migration in C. elegans. Mol. Cell 4: 851–858. https://doi.org/10.1016/S1097-2765(00)80394-9

Whitehurst, A. W., 2014   Cause and Consequence of Cancer/Testis Antigen Activation in Cancer. Pharmacol. Toxicol. 54: 251–272.

Wu, X., Z. Shi, M. Cui, M. Han, and G. Ruvkun, 2012   Repression of Germline RNAi Pathways in Somatic Cells by Retinoblastoma Pathway Chromatin Complexes. PLoS Genet. 8: e1002542. https://doi.org/10.1371/journal.pgen.1002542

Xu, Y., C. Wang, Y. Zhang, L. Jia, and J. Huang, 2015   Overexpression of MAGE-A9 is predictive of poor prognosis in epithelial ovarian cancer. Sci. Rep. 5: 12104. https://doi.org/10.1038/srep12104

Yang, Y., and M. Mlodzik, 2015   Wnt-Frizzled/planar cell polarity signaling: cellular orientation by facing the wind (Wnt). Annu. Rev. Cell Dev. Biol. 31: 623–646. https://doi.org/10.1146/annurev-cellbio-100814-125315

Yan, D., J. B. Wallingford, T.-Q. Sun, A. M. Nelson, C. Sakanaka *et al.*, 2001   Cell autonomous regulation of multiple Dishevelled-dependent pathways by mammalian Nkd. Proc. Natl. Acad. Sci. USA 98: 3802–3807. https://doi.org/10.1073/pnas.071041898

Yakirevich, E., E. Sabo, O. Lavie, S. Mazareb, G. C. Spagnoli *et al.*, 2003   Expression of the MAGE-A4 and NY-ESO-1 Cancer-Testis Antigens in Serous Ovarian Neoplasms. Clin. Cancer Res. 9: 6453.

Zhao, Y., C.-H. Tan, A. Krauchunas, A. Scharf, N. Dietrich *et al.*, 2018   The zinc transporter ZIPT-7.1 regulates sperm activation in nematodes. PLoS Biol. 16: e2005069. https://doi.org/10.1371/journal.pbio.2005069

Zwamborn, R., C. Snijders, N. An, A. Thomson, B. Rutten *et al.*, 2018   Chapter Seven - Wnt Signaling in the Hippocampus in Relation to Neurogenesis, Neuroplasticity. Stress and Epigenetics. 158: 129–157.

Communicating editor: A. Walhout

G3 Genes | Genomes | Genetics